



Contents lists available at ScienceDirect

Quaternary Science Reviews

journal homepage: www.elsevier.com/locate/quascirev

Constraints on Lake Agassiz discharge through the late-glacial Champlain Sea (St. Lawrence Lowlands, Canada) using salinity proxies and an estuarine circulation model

Brandon Katz^a, Raymond G. Najjar^{a,*}, Thomas Cronin^b, John Rayburn^c, Michael E. Mann^a

^a Department of Meteorology, 503 Walker Building, The Pennsylvania State University, University Park, PA 16802, USA

^b United States Geological Survey, 926A National Center, 12201 Sunrise Valley Drive, Reston, VA 20192, USA

^c Department of Geological Sciences, State University of New York at New Paltz, 1 Hawk Drive, New Paltz, NY 12561, USA

ARTICLE INFO

Article history:

Received 30 January 2011

Received in revised form

25 July 2011

Accepted 5 August 2011

Available online xxx

Keywords:

Champlain sea

Proglacial lakes

Paleosalinity

ABSTRACT

During the last deglaciation, abrupt freshwater discharge events from proglacial lakes in North America, such as glacial Lake Agassiz, are believed to have drained into the North Atlantic Ocean, causing large shifts in climate by weakening the formation of North Atlantic Deep Water and decreasing ocean heat transport to high northern latitudes. These discharges were caused by changes in lake drainage outlets, but the duration, magnitude and routing of discharge events, factors which govern the climatic response to freshwater forcing, are poorly known. Abrupt discharges, called floods, are typically assumed to last months to a year, whereas more gradual discharges, called routing events, occur over centuries. Here we use estuarine modeling to evaluate freshwater discharge from Lake Agassiz and other North American proglacial lakes into the North Atlantic Ocean through the St. Lawrence estuary around 11.5 ka BP, the onset of the Preboreal oscillation (PBO). Faunal and isotopic proxy data from the Champlain Sea, a semi-isolated, marine-brackish water body that occupied the St. Lawrence and Champlain Valleys from 13 to 9 ka, indicate salinity fell about 7–8 (range of 4–11) around 11.5 ka. Model results suggest that minimum (1600 km³) and maximum (9500 km³) estimates of plausible flood volumes determined from Lake Agassiz paleoshorelines would produce the proxy-reconstructed salinity decrease if the floods lasted <1 day to 5 months and 1 month to 2 years, respectively. In addition, Champlain Sea salinity responds very quickly to the initiation (within days) and cessation (within weeks) of flooding events. These results support the hypothesis that a glacial lake flood, rather than a sustained routing event, discharged through the St. Lawrence Estuary during the PBO.

© 2011 Elsevier Ltd. All rights reserved.

1. Introduction

During the last retreat of the Laurentide Ice Sheet, large proglacial lakes formed from precipitation and meltwater along the southern margin of the ice sheet. Lake Agassiz was the largest of these lakes, covering up to 1.5 million km² in the northern plains of North America during its 5000-year history (Leverington and Teller, 2003; Teller and Leverington, 2004). Other lakes, such as Lake Algonquin, occupied the current Great Lakes region, and Lake Iroquois and Lake Vermont occupied the Ontario–St. Lawrence–Champlain Valley region (Fig. 1). North American proglacial lakes have a complex history governed by precipitation, variable meltwater rates, and the opening of various outlet channels due to

isostatic rebound and the position of the retreating ice sheet margin (Licciardi et al., 1999).

One hypothesis to explain widespread paleoclimatic evidence for abrupt climatic cooling events during the last deglacial interval (~19–11.5 ka BP¹) involves the abrupt discharge of large volumes of meltwater from proglacial lakes into subpolar regions of the North Atlantic Ocean (Johnson and McClure, 1976; Broecker et al., 1989; Clark et al., 2001). Climate models have been used for studying the potential for a mechanistic link between meltwater discharge events and subsequent changes in ocean circulation and climate. Such models, however, vary widely in their sensitivity to meltwater events (Stouffer et al., 2006). Some climate models indicate that abrupt freshwater discharges over one year or less

* Corresponding author. Tel.: +1 814 863 1586; fax: +1 814 865 3663.
E-mail address: najjar@meteo.psu.edu (R.G. Najjar).

¹ BP = Before Present. Unless otherwise specified, all dates are calendar dates, not radiocarbon dates.

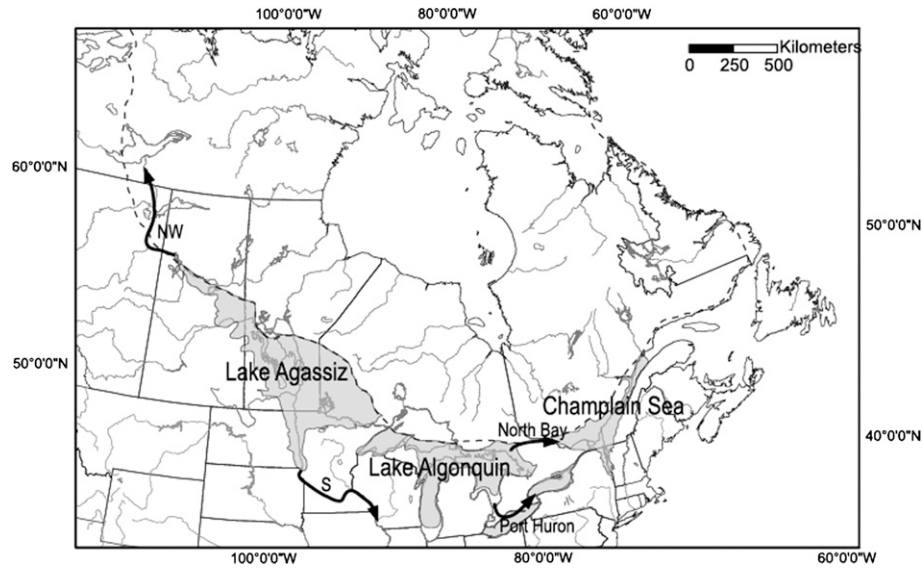


Fig. 1. Map of the proglacial lake system around 11.5 ka BP. The dashed line represents the southern boundary of the Laurentide Ice Sheet, the darker gray portions depict the water-bodies, and arrows delineate theorized drainage routes proposed by Teller and Leverington (2004). Not all routes discussed in text are shown on this figure. Modified from Cronin et al. (2008b).

might catalyze abrupt climate change by freshening the surface ocean, which would decrease the strength of Atlantic Meridional Overturning Circulation (AMOC) and result in widespread cooling (Ganopolski and Rahmstorf, 2001; Rahmstorf, 2002; Rahmstorf et al., 2005; LeGrande et al., 2006). Some of these models are characterized by multiple equilibria (hysteresis) of the AMOC, and are more susceptible to short-term changes in freshwater forcing. Other models show a lack of hysteresis and are more consistent with the view that gradual re-routing of freshwater drainage over centuries and millennia has a greater potential for weakening the AMOC and causing a climatic cooling (Meissner and Clark, 2006; Liu et al., 2009).

Understanding freshwater forcing of climate is important in gauging the potential for abrupt climate changes in response to future changes in the hydrological cycle in high latitudes resulting from anthropogenic warming (Rawlins et al., 2010). Such increases in freshwater flux are expected to occur in response to the melting of the Greenland and Antarctic Ice Sheets (Overpeck et al., 2006) and river runoff resulting from the intensification of the hydrological cycle (Milly et al., 2005). Though some have argued that the AMOC is unlikely to be strongly influenced by future climate change (Weaver and Hillaire-Marcel, 2004), recent modeling studies show consensus in weakening of the AMOC under greenhouse warming, with the weakening resulting more from changes in heat flux than in freshwater flux (Gregory et al., 2005; Meehl et al., 2007; Yin et al., 2009). Furthermore, Hofmann and Rahmstorf (2009) suggested that the current generation of climate models overestimates the stability of the AMOC. The current uncertainty about future AMOC changes underscores the importance of understanding how the ocean has responded in the past to freshwater inputs.

Five major flood routes have been proposed for as many as 19 distinct Agassiz discharge events: southward through the current-day Mississippi River Valley to the Gulf of Mexico, through the Mackenzie River Valley to the Arctic Ocean, through Hudson Bay and Hudson Strait into the North Atlantic Ocean, and two routes into the North Atlantic through the Hudson and St. Lawrence River Valleys (Leverington and Teller, 2003; Fig. 1). Teller et al. (2002, and references therein) speculated that most, if not all, of the main

Agassiz lake-level drops occurred within a time period of months to years and geomorphic evidence indicates that some discharge events may have been catastrophic, often scouring out deep gorges and valleys. However, geomorphic and stratigraphic records are not sufficient to accurately constrain the duration of discharge events. More generally, the timing, magnitude and location of most post-glacial flood events, critical factors for how they influence ocean circulation and climate (Meissner and Clark, 2006), are still poorly known (Lowell et al., 2005) and paleoceanographic evidence for freshwater influx is still debated (Weaver and Hillaire-Marcel, 2004; Ellison et al., 2006; Carlson et al., 2007). Such uncertainties have posed a challenge to using these paleoclimate analogs to inform our understanding of the relationship between freshwater forcing and the AMOC.

Our study focuses on the St. Lawrence-Champlain Valleys, which have long been viewed as an outlet route for several flood events, including that which may have caused the Younger Dryas cooling event about 13.0 ka (Broecker et al., 1989). Following the drainage of Lake Vermont about 13.1 ka, the isostatically depressed St. Lawrence-Champlain Valleys were inundated by marine water forming the estuary-like Champlain Sea (Hillaire-Marcel and Occhietti, 1977; Parent and Occhietti, 1988; Rayburn et al., 2005, 2006; Franzi et al., 2007). The estuarine character of this sea was likely maintained by runoff generated from precipitation, which Licciardi et al. (1999) estimated to be substantial based on an atmospheric general circulation model. Sediment records indicate substantial salinity fluctuations in the Champlain Sea, but it is still unclear what their causes were and if they signify freshwater influx from glacial lakes to the west (Rodrigues, 1988; Rodrigues and Vilks, 1994; de Vernal et al., 1996; Moore et al., 2000; Clark et al., 2001; Carlson et al., 2007; Cronin et al., 2008b). The paleosalinity record of the Champlain Sea may be viewed as a kind of uncalibrated freshwater flux gage, providing qualitative evidence for freshwater influx and dilution of marine water in this paleo-estuary.

Studies of modern estuaries show a strong link between riverine input and salinity (e.g., Schubel and Pritchard, 1986), and process-based estuarine dynamical models are generally able to capture this relationship (e.g., Li et al., 2005). Here we bring to bear the tools of estuarine dynamics to the problem of relating Champlain Sea

salinity variations to the freshwater flows that may have caused them. The study focuses on a widespread fall in salinity about 11.5 ka BP (Franzi et al., 2007; Cronin et al., 2008a, 2008b), an age preceding the brief climate cooling event in the North Atlantic region called the Preboreal Oscillation (PBO). We use the model to test the hypothesis that the observed Lake Agassiz volume drops could have been responsible for the observed Champlain Sea salinity decreases. We then further estimate the range of flood durations consistent with these observations. To our knowledge, this is the first attempt to combine estuarine dynamical models with paleosalinity reconstructions and estimates of glacial lake volume to evaluate the drainage of proglacial lake water to the sea.

The remainder of the paper is organized as follows. We first briefly summarize the faunal and isotopic evidence for a freshening event in the Champlain Sea around 11.5 ka BP. We then describe an estuarine dynamical model of the Champlain Sea, present model simulations of the response of the Champlain Sea to floods of varying magnitude and duration, and finally place the results into the context of estimated volume changes of proglacial lakes.

2. Champlain Sea paleosalinity

Numerous studies of Champlain Sea paleosalinity have been conducted using benthic foraminifer and ostracode assemblages (Cronin, 1977, 1979; Hunt and Rathburn, 1988; Guilbault, 1989, 1993; Rodrigues, 1992; Rodrigues and Vilks, 1994), stable isotopes on mollusks (Hillaire-Marcel, 1988) and benthic foraminifers (Corliss et al., 1982; Cronin et al., 2008b; Rayburn et al., 2011), and trace element concentrations (Brand and McCarthy, 2005; Rodrigues, 2006). A large salinity decrease is evident from several proxy records in most regions of the Champlain Sea (Table 1). Rodrigues and Vilks (1994) proposed a large drop in salinity based on their foraminiferal zones R3 and F3; lower salinity also characterized foraminiferal zone B of Guilbault (1989) and ostracode zone B1 of Hunt and Rathburn (1988). The most consistent manifestation of this salinity event is the transition in benthic foraminifers from assemblages dominated by *Elphidium excavatum* forma *clavatum* to those with common *Elphidium albiumbilitatum*. Similar changes occur in ostracode assemblages (Cronin, 1981; Hunt and Rathburn, 1988).

Table 1

Salinity drop derived from changes in $\delta^{18}\text{O}$ from two benthic species in eight cores at seven sites within the Western Champlain Sea (Cronin et al., 2008a). Salinity change is derived using the equations of Fairbanks (1982) and Hoefs (1992). Site data are given in Guilbault (1989, 1993) and for the Melo sites in Cronin et al. (2008b).

Site	Lat (°N)	Long (°W)	Horizons sampled	Species	Salinity drop	
					Fairbanks	Hoefs
St-Césaire	45.41	73.02	6	<i>Haynesina orbiculare</i>	6.5	8.1
St-Césaire	45.41	73.02	3	<i>E. excavatum clavatum</i>	4.8	6.0
Ile Perrot	45.40	73.97	3	<i>E. excavatum clavatum</i>	5.1	6.4
St. Alban (core 1)	46.72	72.08	4	<i>E. excavatum clavatum</i>	8.3	10
St. Alban (core 2)	46.72	72.08	4	<i>E. excavatum clavatum</i>	8.8	11
Verchères	45.78	73.35	3	<i>E. excavatum clavatum</i>	7.1	8.9
St-Roch-de- Richelieu	46.11	73.02	3	<i>E. excavatum clavatum</i>	7.2	9.0
Melo-5	44.17	73.38	14	<i>E. excavatum clavatum</i>	7.1	8.9
Melo-6	44.18	73.38	19	<i>E. excavatum clavatum</i>	4.5	5.6
Mean					6.6	8.2

Cronin et al. (2008b) attempted to quantify the fall in salinity on the basis of oxygen isotopic composition of benthic foraminiferal shells ($\delta^{18}\text{O}_{\text{foram}}$) in sediment cores from the southern arm of the Champlain Sea in the modern Lake Champlain. The paleodepths at these sites were approximately 20–100 m based on the calcareous microfaunal assemblages and the elevation of the site with respect to Champlain Sea paleoshorelines. Using the relationship between modern $\delta^{18}\text{O}$ of ocean water and salinity in Labrador Slope Water (Fairbanks, 1982), $\delta^{18}\text{O}_{\text{foram}}$ -derived mean values for the decrease in salinity are 7.1 and 4.5 for sediment cores Melo-5 and Melo-6, respectively (Table 1). The more general salinity/ $\delta^{18}\text{O}$ relationship of Hoefs (1992) gives a slightly larger salinity decrease (8.9 and 5.6, respectively). Recently obtained $\delta^{18}\text{O}_{\text{foram}}$ records from sites in the central Champlain Sea in Quebec and Ontario studied by Guilbault (1989, 1993) suggest a salinity drop between 4.8 and 8.8 using the Fairbanks (1982) equation (Table 1; Cronin et al., 2008a). Considering the multiple sites and two salinity/ $\delta^{18}\text{O}$ relationships, we estimate that the salinity drop was between 4 and 11, with a best estimate of 7–8, the midpoint of the range. Salinity prior to the event has been estimated to be about 25 (Cronin et al., 2008b). These salinity estimates are consistent with qualitative estimates based on the faunal assemblage data showing a shift from marine to brackish water faunas.

The age and duration of the Champlain Sea salinity event are important for evaluation of model simulations and establishing its relationship to glacial lake drainage and climate oscillations. The stratigraphic position of these faunal changes places it roughly in the middle of the Champlain Sea episode. Calendar-year chronology is difficult to establish in Champlain Sea sediments due to reservoir effects on radiocarbon dates on mollusks (Richard and Occhietti, 2005). However, dates on plant material from sediment cores in the southern Champlain Sea give an age of about 11.2–11.4 ka BP (Cronin et al., 2008b). Pending further dating, we assume on the basis of faunal assemblages and stratigraphic position that the salinity event was roughly synchronous throughout the entire Champlain Sea basin. The duration of the salinity event is estimated from core Melo-6 in modern lake Champlain, where reduced salinity persisted for about 80 years assuming a sedimentation rate of 1 cm yr^{-1} (Cronin et al., 2008b).

3. Model and observational constraints

3.1. Estuarine model

Evaluating the causes of salinity change in the Champlain Sea requires an estuarine model that is complex enough to contain the essential dynamics thought to be important for the Champlain Sea and yet has enough computational speed for exploring a wide range of possible flood magnitudes and durations. The latter constraint makes 3-dimensional models infeasible for this study. Rodrigues and Vilks (1994) suggested that the Champlain Sea has important salinity and flow gradients in two dimensions: along the main axis of the estuary and with depth. For this reason, we chose the two-dimensional model of MacCreedy (2007), which is a dynamical model capable of simulating estuarine velocity and salinity distributions averaged over a tidal cycle. The model is essentially a time-dependent version of the analytical model of Hansen and Rattray (1965). The tidal mixing parameterization of the model was developed and optimized using characteristics from real-world estuaries. The model gives reasonable salinity and flow profiles for San Francisco Bay, Hudson Bay, and several other estuaries.

The model assumes a horizontal force balance between tidal mixing and the pressure gradient force, which means that wind mixing and momentum advection are relatively unimportant.

Ignoring wind mixing is likely reasonable, given the fact that wind mixing is at most 5% of tidal mixing in the modern St. Lawrence Estuary (Saucier and Chassé, 2000). We can roughly evaluate the assumption of ignoring momentum advection in the modern St. Lawrence estuary by a scale analysis that compares $u\partial u/\partial x$ with the pressure gradient force resulting from the salinity gradient, $gz\beta\partial S/\partial x$, where u is the horizontal velocity, x the along-axis distance, g the acceleration due to gravity, z the depth, β the haline contraction coefficient, and S the salinity. The ratio of the two terms is approximately $u^2/gz\beta S$, where u and S are now velocity and salinity scales, taken to be 1 m s^{-1} and 10, respectively (Saucier and Chassé, 2000). Then, with $\beta \sim 10^{-3}$, $z \sim 100\text{ m}$, and $g \sim 10\text{ m s}^{-2}$, we find that momentum advection is about an order of magnitude smaller than the pressure gradient force. Thus, the model appears to be a reasonable choice for application to the Champlain Sea.

Required inputs to the model are bathymetry, salinity and daily averaged tidal velocity at the mouth of the estuary (the ocean boundary), and freshwater influx at the head of the estuary. The model assumes a simplified bathymetry in which the cross section is rectangular. In this configuration, the depth is equal to the maximum depth and the width is computed in order to maintain the observed cross-sectional area. Spatial resolution for the model is 20 km along the axis of the estuary and continuous in the vertical. The time step is variable, adjusting to flow changes in order to maintain numerical stability while minimizing computational expense.

3.2. Bathymetric reconstruction

In order to create the bathymetric profile for the 11.5 ka salinity event, several sources of information were combined: nautical charts of the current-day St. Lawrence Seaway, a Digital Elevation Model (DEM) of the St. Lawrence region, DEM reconstructions of the Champlain Sea Region during the event, and the location of the southern boundary of the Laurentide Ice Sheet.

The nautical charts were obtained from the Defense Mapping Agency and Hydrographic/Topographic Center in Bethesda, MD². The maps display high-resolution ship soundings of depth from Mean Lower Low Water (MLLW, the average of the lower of the two low tides each day), which can easily be read and transcribed into a data file. These charts were used instead of digital sources because of their higher resolution (10-m depth spaced contours compared to 2-km blocks). To determine where to sample depth information, a transect was overlaid running from the mouth of the waterway at 65° W to Quebec City (71° W). At intervals of 20 km, lines were drawn perpendicular to the primary flow axis from the center of the waterway to the coasts. Depth was then recorded at 7.5-km intervals from the north coast to the south coast. In more variable bathymetry or where the width is less than 75 km, the resolution was increased by progressively halving the 7.5-km spacing so that at least ten points are present in each cross-section. The finest spacing used is 0.9375 km.

Elevation above water level around the St. Lawrence was derived from the current-day DEM of the St. Lawrence region, obtained from the National Geophysical Data Center (Amante and Eakins, 2008). The flow axis and perpendicular transects were again overlaid on the DEM with the location of the north and south coasts (the limits of the nautical charts) plotted. Elevations were recorded to the north and south of the coasts at the same resolution as the nautical chart transects. In order to link the current-day DEM with the nautical charts, readings were taken at each perpendicular

transect's coastlines and the DEM was then corrected to the nautical chart. Fig. 2 depicts this method. The result is a single consistent topographic and bathymetric data set for the current-day St. Lawrence Region.

Because of the weight of the Laurentide Ice Sheet, the St. Lawrence–Champlain Valleys were isostatically depressed during the time period of interest. Furthermore, global mean sea level was lower than today due to the storage of water in continental ice sheets. To account for these isostatic and sea-level effects, a reconstructed DEM (referred to as a paleo-DEM throughout) of the western portion of the Champlain Sea at 11.5 ka BP was obtained from Rayburn et al. (2005) (see Fig. 3a). They used modern DEMs, paleo-strandlines (ancient beaches and deltas that determine coastlines), and isostatic rebound lines to produce the differentially depressed topography and bathymetry of the western Champlain Sea. By selecting a point on the paleo-DEM that is closest and overlapping to the St. Lawrence Region (the most northeast corner of the paleo-DEM), the same operation depicted in Fig. 2 was performed to correct the current-day combined topography/bathymetry of the St. Lawrence Region to 11.5 ka BP. The water level of Rayburn et al. (2005) was then used for the combined DEM. This corrected DEM is shown in Fig. 3b and will be referred to as the Modified Period DEM (MPD).

The primary flow axis and transects are now extended from Quebec City to 75° W in the Champlain Sea. For perpendicular transects that overlap both the paleo-DEM and the MPD (i.e. that run northward outside of the boundary defined by the northern border of the paleo-DEM), the operation depicted in Fig. 2 was used to correct the portion of the transect within the MPD to the portion of the transect within the paleo-DEM. After adjusting the overlapping transects, the location of the Laurentide Ice Sheet was considered as it may have formed sections of the waterway's northern boundary. The latitudes and longitudes of the ice sheet boundaries were obtained from Dyke et al. (2003) and subsequently drawn onto the DEM, with the 10,000 radiocarbon years BP map used for the 11.5 ka BP event (Rayburn et al., 2005); see Fig. 3b.

The bathymetric data set created in this way was then used to determine the maximum depth and cross-sectional area at each transect perpendicular to the main axis of the estuary. The cross-sectional area was computed using trapezoidal integration, and is shown in Fig. 4. The total volume of the estuary for the 11.5 ka BP event is $8.45 \times 10^5\text{ km}^3$.

3.3. Estuarine model pre-flood configuration

For the model to simulate steady-state, pre-flood conditions, the background (i.e., pre-flood) freshwater flow at the head of the estuary, and ocean boundary salinity and daily averaged tidal velocity are needed. Two estimates of the background freshwater flow are used, which are based on estimates of precipitation during the period, the Laurentide Ice Sheet's melt rates, extensive field

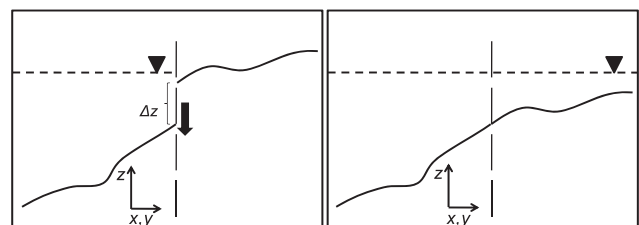


Fig. 2. Graphical depiction of map correction technique. One relative profile is assumed to be correct while the other is assumed to require an adjustment to the correct level. The difference between the profiles at the overlapping point, Δz , is subtracted from the second profile.

² Ten maps were used, one published in 1984 (Map ID 14260) and the remainder published in 1995 (Map IDs 14223, 14225–14228, and 14240–14243).

Elevation (m)

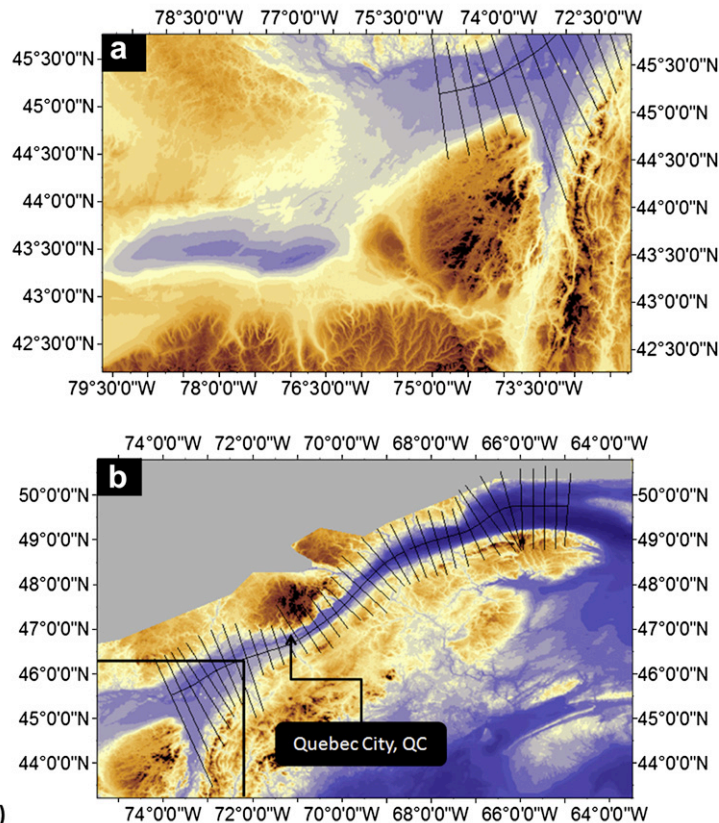
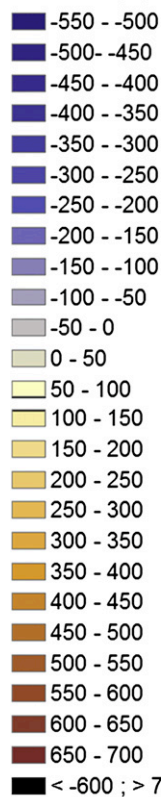


Fig. 3. (a) 11.5 ka BP western Champlain Sea Digital Elevation Model (DEM) of St. Lawrence-Champlain Valleys (from Rayburn et al., 2005). (b) 11.5 ka BP Modified Period DEM (MPD). Transects along the middle of the estuaries represent the primary axis of flow while the perpendicular transects represent the discrete 20-km spaced cross-sections where depths and elevations were recorded. The partial black box visible in the southwestern corner of the MPD is the outline of the western Champlain Sea DEM. The darker gray boundary to the north represents the approximate location of the Laurentide Ice Sheet.

mapping of the Agassiz shorelines and sediments, and estimates of the total volume of proglacial Lake Agassiz, the source of most freshwater to the Champlain Sea (Licciardi et al., 1999; Teller et al., 2002). The lower estimate is $34,000 \text{ m}^3 \text{ s}^{-1}$ or 0.034 Sv ($1 \text{ Sv} = 1 \text{ Sverdrup} = 10^6 \text{ m}^3 \text{ s}^{-1}$) and is based on Teller et al. (2002) (see their Table 1); the higher estimate, 0.1 Sv , is based on Licciardi et al. (1999) and is a rough average of the total runoff to the St. Lawrence for the period 13.5 to 10.6 ka (see their Appendix A). For reference, the lower and higher estimates are, respectively, 4.9 and

14 times the average flow of the modern St. Lawrence River at Ogdensburg, New York (Pekárová et al., 2003). The lower estimate is only from Lake Agassiz and is likely a lower bound of the freshwater flow to the Champlain Sea, which would also include runoff from the Great Lakes watershed (Licciardi et al., 1999; Teller et al., 2002).

The value for salinity at the open-ocean boundary is assumed to be constant at 30, similar to the current-day annual-mean salinity in the Gulf of St. Lawrence (Koutitonsky et al., 2002). Using the estimates for baseline freshwater flow and ocean boundary salinity, the daily averaged tidal velocity, which is not known for the past, may then take the place of a tuning parameter. The tidal velocity was varied until the salinity of the Champlain Sea (specifically, at the location of the cores analyzed by Cronin et al., 2008b) equaled the observed value (~ 25 , see Section 2 above). With initial conditions satisfied, the model was then run using varying flood magnitudes and durations derived from the geologic evidence presented in the next section.

3.4. Description of flooding simulations

Individual volume discharges from Lake Agassiz were estimated by Teller et al. (2002) to range from 1600 to 9500 km^3 between 9 and 11 ka radiocarbon years, which equates to about 10–13 ka calibrated years. The outlets of many of these floods were directed toward the east, likely through the region inundated by the Champlain Sea. In

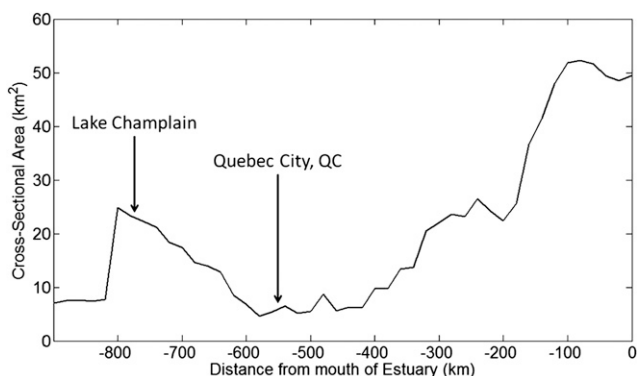


Fig. 4. Along-axis cross-sectional area of the estuary. The current-day locations of Lake Champlain and Quebec City are shown.

order to test the full parameter space of salinity change vs. flood duration and magnitude, 7 flood volumes were run for 20 flood durations and were added to each of the two background freshwater flows (the higher and lower flow rates), which makes a total of 280 simulations. Two of the flood volumes are 1600 and 9500 km³. The other five are 0.05, 0.1, 1, 10 and 20 times 3700 km³, which is the volume of one of the medium-sized, eastward-routed, early-Holocene floods estimated from Lake Agassiz strandline data by Teller et al. (2002). The seven flood volumes are therefore 185, 370, 1600, 3700, 9500, 37,000, and 74,000 km³. For reference, these volumes vary from 0.02% to 9% of the volume of the Champlain Sea. These volumes are each spread out evenly over times of one day, two days, seven days, fourteen days, one to twelve months in monthly increments, and two to five years in yearly increments. Thus, depending on the duration and magnitude of the flood, flow rates for these floods vary by nearly six orders of magnitude, from $1.2 \times 10^3 \text{ m}^3 \text{ s}^{-1}$ to $8.6 \times 10^8 \text{ m}^3 \text{ s}^{-1}$; compare this with the lower and higher background freshwater flows $3.4 \times 10^4 \text{ m}^3 \text{ s}^{-1}$ and $1 \times 10^5 \text{ m}^3 \text{ s}^{-1}$. As mentioned above, Teller et al. (2002) estimated that the floods occurred in about 1 year, but the dimensions of the paleo-channels through which floods discharged is unknown, and thus an exact flow rate cannot be estimated from channel geomorphology and hydraulic equations. Our wide range of flow rates accounts for this uncertainty. All simulations begin with 80 days spinup at the background freshwater flow to achieve a steady state, followed by a flooding period, and then a return to the background flow. The total duration of the simulations is 2 years for floods less than 1 year and 7 years for floods 2–5 years. We admit that floods lasting a year or more may be affected by seasonal ice jamming and breakup, but this is a factor we did not consider.

4. Results and discussion

4.1. Pre-flood simulations

To achieve a pre-flood salinity (S_p) of 25 in the western Champlain Sea in the presence of the lower background freshwater flow (0.34 Sv), a tidal velocity of 3.05 m s^{-1} was required. With the higher background freshwater flow (0.1 Sv), the tidal velocity had to be decreased to 2.10 m s^{-1} to obtain the same initial conditions. This decrease in tidal velocity is expected because increased freshwater forcing at the head of the estuary increases the amount of salt-water intrusion needed to maintain the aforementioned pre-flood salinity distribution, which is inversely proportional to tidal velocity. Unfortunately, there are no estimates of tidal velocity in the Champlain Sea with which to compare our estimates from model tuning, though we can compare with the modern St. Lawrence: recent observations show tidal velocity varying spatially from about 0.5 to 2 m s^{-1} (Saucier and Chassé, 2000).

Fig. 5 shows the pre-flood steady state distributions of salinity and velocity for the two background freshwater flow cases (0.034 and 0.1 Sv). Both cases display typical estuarine flow dynamics, with fresher, seaward flow in near-surface water and saltier, landward flow at greater depths. The lower background freshwater flow case has a larger tidal velocity, and thus is seen to be more vertically mixed with weaker flows, whereas the higher background freshwater flow case has a weaker tidal velocity, greater stratification, and stronger flows. The simulated salinity and flow distributions are remarkably similar to those hypothesized for the Champlain Sea by Rodrigues and Vilks (1994, their Fig. 14).

4.2. Flood simulations

Fig. 6 shows the evolution of simulated salinity in the western Champlain Sea at depths of 20 and 100 m in response to a 3700-

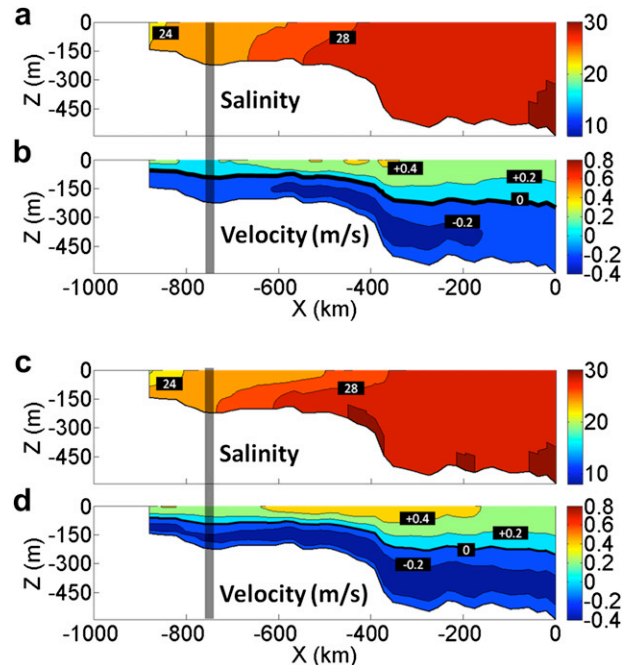


Fig. 5. Steady-state pre-flood salinity (a and c) and velocity (b and d) as a function of distance from the ocean and depth. Each pair corresponds to a different baseline freshwater flow: the upper panels (a and b) use 0.034 Sv (Teller et al., 2002) while the lower panels (c and d) use 0.1 Sv (Licciardi et al., 1999). The heavy black line on the velocity plot denotes the boundary between positive (seaward) and negative (landward) flow velocities. Contour intervals are 4 for salinity and 0.2 m s^{-1} for velocity. The gray bar indicates the region where paleosalinity values of 25 from Cronin et al. (2008b) are located.

km³ flood released over one day, two months, and one year on top of the lower background freshwater flow rate (0.034 Sv). The flow rates for these floods range from 3 to 1300 times the background freshwater flow. The maximum salinity drop occurs near the surface at the 20-m level with a total salinity change of 25 (complete freshening) for the 1-day flood, 10 for the 2-month flood, and 3.8 for the 1-year flood. Salinity falls as soon as the flood begins (day 80) and approaches the pre-flood value in a quasi-exponential manner immediately after the flood ends. An estimate of the characteristic response time (or e -folding time) for returning to pre-flood salinity ($S_p = 25$) can be made by determining the time it takes the salinity to go from its minimum value (S_m) to $S_p - (S_p - S_m)/e$. At 20 m, the response times for floods of 1 day, 2 months and 1 year are 12, 36, and 78 days, respectively, while the corresponding times at 100 m are 34, 36, and 66 days. For large floods (volumes greater than 3700 km³), the range of recovery times for both depths and all durations is 12–96 days. The response time for the re-salinization of the estuary after the flood event generally decreases with flood duration. This makes sense because the residual circulation of an estuary increases with the volumetric flow rate of its freshwater forcing (and therefore decreases with the duration of a flood of a given volume); a stronger residual circulation means a shorter residence time for water parcels in an estuary and therefore a more rapid return to steady state.

Fig. 7 shows the simulated salinity and velocity for the estuary at the end of the 3700-km³ flood that lasts for one month (corresponding to Fig. 6c and d). Compared to pre-flood conditions (Fig. 5a), salinity drops everywhere except for bottom waters in the central and seaward portions of the estuary, which become saltier or remain at a salinity of 30. The vertical salinity gradient increases as well, with the surface-to-bottom difference exceeding 20 at

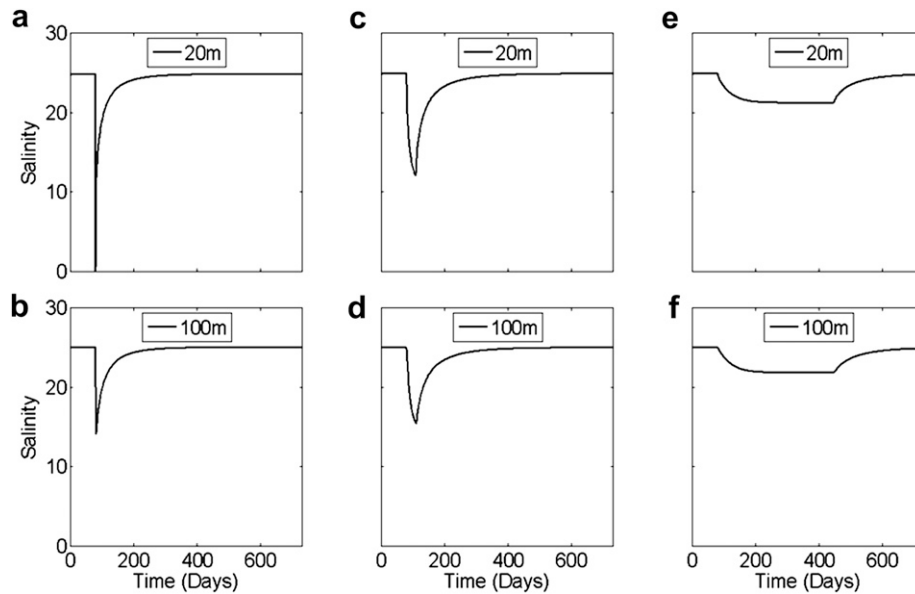


Fig. 6. Simulated salinity change in the western Champlain Sea vs. time resulting from a 3700-km³ flood. The background freshwater flow is 0.034 Sv. Salinity change is shown at depths of 20 m (a, c, and e) and 100 m (b, d, and f). The horizontal location of the site is given by the gray bar in Fig. 5. The flood occurs over one day in panels a and b, 1 month in panels c and d, and one year in panels e and f.

some locations. The structure of the velocity field, exhibiting a classical residual circulation pattern for a partially mixed estuary, remains unchanged from pre-flood conditions (Fig. 5c), but the magnitude of the circulation has increased by about a factor of three. The increase in landward flow at depth explains the bottom-water salinity increase.

Fig. 8 shows, as a function of flood volume and duration, the maximum salinity drop in the western Champlain Sea at 20 and 100 m water depth for the two background freshwater flow rates (0.034 and 0.1 Sv). In general, the salinity drop increases with flood volume, decreases with flood duration, and decreases with depth. The figure outlines the range of salinity decreases of 4–11 from the sediment core proxy records discussed above (see Table 1 and Section 2), as well as the range in flood magnitudes corresponding to Lake Agassiz level drops for the early Holocene, 1600–9500 km³ (Teller et al., 2002). The overlap of the two regions shows that many of the simulations conducted are consistent with the available constraints on both the size of Champlain Sea proxy-derived salinity changes and Lake Agassiz volume changes. For a flood of a specific volume, one can determine the range of durations consistent with the estimated salinity change. For example, for

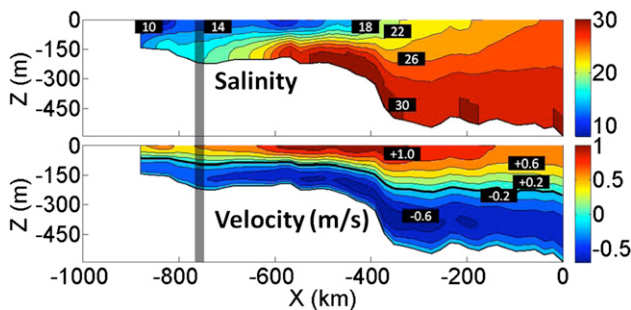


Fig. 7. Model salinity and velocity 30 days after the beginning of the 30-day, 3700-km³ flood. The lower background flow rate is used here. The highlighted area is the location of cores in the western Champlain Sea from Cronin et al. (2008b). The black line in the velocity cross-section delineates between positive and negative flow values. This figure can be compared with Fig. 5. Note that the salinity color scale is the same as in Fig. 5, but the velocity scale has been changed.

a flood of 9500 km³, which is at the high end of Lake Agassiz flood range for this time period, the flood duration must be between 66 and 330 days, assuming that the salinity proxy data reflect changes at 20 m water depth, and that the background flow was 0.1 Sv. At 100 m the durations are shorter because the salinity drop is smaller.

Under the higher background freshwater flow, the maximum salinity drop for a given flood volume is lower than the drop under the lower background flow (Fig. 8c and d, compare to Fig. 8a and b). This change is expected because the total estuarine circulation strengthens as the freshwater influx is increased, which has the effect of retaining the freshwater signal in the estuary for a shorter time and thereby preventing salinity from dropping further. For a similar reason, the recovery times decrease when the background flow rate increases. Finally, due to weaker tidal mixing, the depth dependence of the salinity change is greater for the increased background freshwater flow case. Because the simulations with higher background freshwater flow have a smaller salinity drop compared with the simulations with the lower background freshwater flow, the flood durations that are consistent with the salinity proxy data are shorter. For example, for a flood of 9500 km³, the allowable flood durations under the higher background flow are about a half to a fifth of those under the lower background flow.

Table 2 summarizes the flood durations that are consistent with the estimated salinity drop of 4–11 (Table 1) over the plausible range of salinity proxy sample depths (20–100 m) for the range of flood volumes suggested by the Teller et al. (2002) Agassiz strandline analysis (1600–9500 km³). The model results suggest that minimum (1600 km³) and maximum (9500 km³) estimates of plausible flood volumes determined from Lake Agassiz paleo-shorelines would produce the observed salinity decrease over timescales of <1 to 140 days and 18 to 880 days, respectively. The corresponding range in freshwater fluxes is 0.1 to >20 Sv for the 1600-km³ flood and 0.1 to 6 Sv for the 9500 km³ flood.

5. Possible sources of error

In addition to uncertainty imposed by the conversion of oxygen isotopes to paleosalinity, there are several possible sources of error

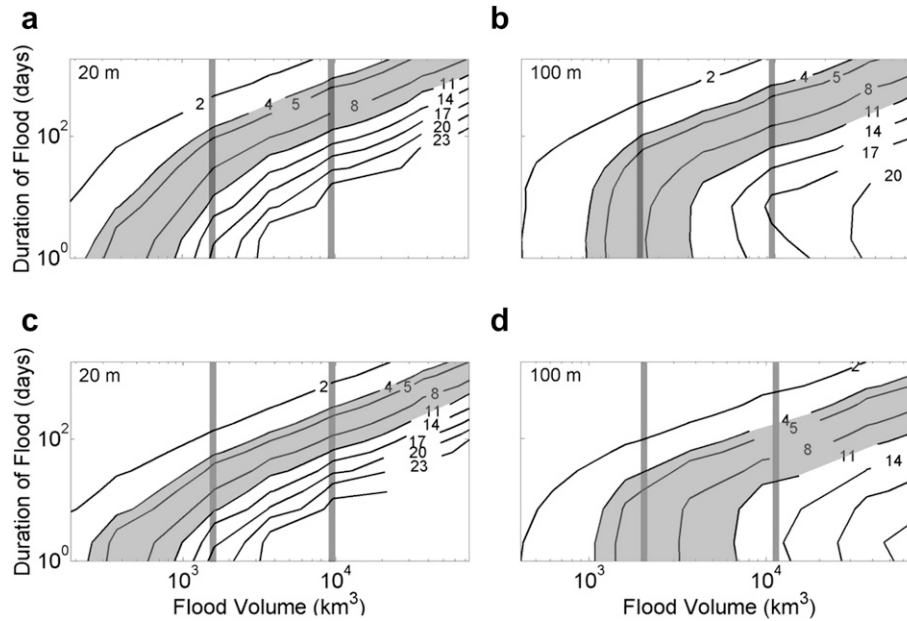


Fig. 8. Maximum salinity change in the western Champlain Sea (indicated by gray bars in Figs. 5 and 7) as a function of flood volume (horizontal axis, km³) and duration (vertical axis, days). Salinity changes are shown for 20 m (left panels: a and c) and 100 m (right panels: b and d) using a background flow of 0.034 Sv (Teller et al., 2002) (upper panels: a and b) and 0.1 Sv (Licciardi et al., 1999) (lower panels: c and d). The vertical bars highlight the range of Lake Agassiz early Holocene floods (Teller et al., 2002). The shaded regions highlight the range of the salinity drop in the Champlain Sea around 11.5 ka BP (Table 1).

in the modeling approach taken here to estimate the duration of eastward flowing floods from North American proglacial lakes through the Champlain Sea: (1) the construction of the bathymetry, (2) the estuarine model, and (3) the estimation of the background freshwater flow. These errors are now discussed in more detail.

One error associated with the bathymetry is the use of a current-day DEM, which assumes that erosion and sedimentation over the past 11 ka have not substantially changed the topographic and bathymetric relief. The isostatically adjusted paleo-DEM of the western Champlain Sea constructed by Rayburn et al. (2005) has potential for additional errors, including those stemming from the paleo-strandline data, which provide information on the coastlines (and therefore depth), and control the estimated isostatic rebound. However, we believe that these DEM-related errors are modest. With regard to strandline data, subsequent mapping by the authors and others (De Simone et al., 2008) has increased confidence in shoreline positions estimated by Rayburn et al. (2005). Rayburn et al. (2005) estimated that the computed volumes have maximum errors on the order of $\pm 15\%$, which would modestly affect the overall modeled circulation and salinity. Small absolute errors in bathymetry in constricted areas could substantially affect model circulation, but it is in precisely such areas where the surface

is expressed as exposed bedrock that the paleobathymetry model would be most accurate.

In combining the nautical charts, the current-day DEM, and the paleo-DEM, the method described in Fig. 2 was used. Because the nautical chart and the current-day DEM both depict the same area at roughly the same time, the relative elevations should require no correction. However, because the current-day DEM averages the elevations within a 2-km grid box, the boxes at the coasts where the maps are connected may see elevation disparities on the order of 1 to 30 m. In this case, error is likely negative in sign, due to the fact that the current-day DEM cross-sections to the north and south of the coasts are corrected for an elevation that is under-predicting the true elevation due to the averaging out of sharp coastal elevation increases.

Connecting the paleo-DEM maps with the nautical chart/current-day DEM results in additional error. This was done as a simple way of modeling isostatic rebound. The error here may not be as large as anticipated because the isostatic rebound lines in the St. Lawrence parallel the coastline of the waterway (Parent and Occhietti, 1988).

Regarding errors in the estuarine model itself, MacCready (2007) notes that it has difficulty in areas where the bottom topography varies greatly over small distances and in places where the waterway is very narrow and shallow. While there are not extreme cases wherein the above constraints are violated, areas of steep bottom slopes do exhibit unusual variations in surface velocities. It is unknown if these are true attributes of the system or artifacts of the model.

Finally, the background freshwater flow values from Teller et al. (2002) and Licciardi et al. (1999) were derived using the total surface area of the ice sheet as well as estimated precipitation over the ice sheet, the latter being particularly uncertain. We showed that a factor of three change in baseline flow can significantly affect the range of possible flood durations (Table 2). This error is very difficult to quantify, and is an area which requires more study to determine its sign and magnitude.

Table 2

Summary of flood durations (in days) consistent with the salinity proxy data from sediment cores (salinity drop between 4 and 11, Table 1) for a given flood volume, background freshwater flow rate, and assumed representative depth of the salinity proxy data. Linear interpolation was used to find flood durations corresponding to salinity drops of 4 and 11.

Flood Volume (km ³)	Teller et al. (2002)		Licciardi et al. (1999)	
	Background Flow		Background Flow	
Depth (m)	1600	9500	1600	9500
20	11–140	130–880	7–55	66–330
100	<1–100	65–680	<1–21	18–160

6. Discussion and conclusions

Our analysis combining salinity proxy data and an estuarine model of the Champlain Sea shows that a wide range of flood volumes and duration are consistent with an observed freshening event around 11.5 ka BP. In short, we have shown that a plausible cause of this freshening event was flooding resulting from an abrupt drainage of water from Lake Agassiz or another North American glacial lake. If the flood was relatively small ($\sim 1600 \text{ km}^3$), then the flood duration was likely between 1 day and 5 months. At the high end of plausible flood volumes ($\sim 9500 \text{ km}^3$), the duration was likely between 1 month and 2 years. Our model simulations suggest that discharge events sustained for longer than a few years, such as the gradual routing of western glacial lake water over centuries, would not have produced salinity changes in the Champlain Sea as large as those reconstructed from the proxy data. In addition, Champlain Sea salinity likely responded very quickly to the initiation and cessation of flooding events, on the order of days to weeks.

The approach taken here is a novel method of estimating the freshwater forcings responsible for observed North Atlantic climate change during the Holocene in regions proximal to the glacial lake water sources, rather than in distal regions in the remote North Atlantic or Arctic Oceans. The location of salinity proxy data in the Champlain Sea is useful in this respect as it implies that the freshwater floods likely flowed for less than a few years out of the current-day Gulf of St. Lawrence into a primary region of upper North Atlantic Deep Water formation in the Labrador Sea. However, our results do not necessarily suggest that abrupt freshwater discharges (floods) were the primary cause of deglacial cooling events nor that sustained freshwater discharges (routing) could not influence the AMOC or climate. Rather, they indicate that it might be difficult to definitively identify lake discharge events in low-resolution paleoceanographic proxy records from open-ocean distal regions due to the rapid salinity response in the case of abrupt events, or the relatively weak signal for routing events. In this sense, they highlight the need for high-resolution records and improved proxy methods in regions close to glacial lake and ice-sheet meltwater sources.

While we believe our analysis to be a novel and useful approach for studying proglacial flood events, a number of improvements are warranted. First and foremost, better constraints on the paleobathymetry are needed. Combining three different map sources into one is far from ideal, and it is difficult to quantify the errors incurred by doing so. A reconstruction of the entire estuary, from current-day Lake Erie to regions outside the Champlain Sea in the modern Gulf of St. Lawrence, would substantially increase the accuracy of the results. An improved estimate (with error bounds) of the baseline freshwater flow rate is also needed because this parameter helps constrain the tidal velocity, the residual circulation, and therefore, the magnitude and character of the estuarine response to flooding. Improved temporal resolution of sediment based proxy records would also improve our understanding of the salinity response to the cessation of freshwater influx. Finally, now that a first-order assessment of the likely phase space of estuarine dynamical parameters has been explored, more realistic, three-dimensional modeling studies would be beneficial.

Acknowledgments

This research was supported by Cooperative Agreement 07ERAG0002 from the United States Geological Survey Global Change Program. We thank Parker MacCready for making his

numerical model available and we are grateful for the comments of two anonymous reviewers.

References

- Amante, C., Eakins, B.W., 2008. ETOPO1 1 Arc-Minute Global Relief Model: Procedures, Data Sources and Analysis. National Geophysical Data Center, NESDIS, NOAA, U.S. Department of Commerce, Boulder, CO (August).
- Brand, U., McCarthy, F.M.G., 2005. The Allerød–Younger Dryas–Holocene sequence in the west-central Champlain Sea eastern Ontario: a record of glacial, oceanographic and climatic changes. *Quaternary Science Reviews* 24, 1463–1478.
- Broecker, W.S., Kennett, J.P., Flower, B.P., Teller, J.T., Trumbore, S., Bonani, G., Wolfli, W., 1989. Routing of meltwater from the Laurentide Ice Sheet during the Younger Dryas cold episode. *Nature* 341, 318–321.
- Carlson, A.E., Clark, P.U., Haley, B.A., Klinkhammer, G.P., Simmons, K., Brook, E.J., Meissner, K.J., 2007. Geochemical proxies of North American freshwater routing during the Younger Dryas cold event. *Proceedings of the National Academy of Sciences* 104, 6556–6561.
- Clark, P.U., Marshall, S.J., Clarke, G.K.C., Hostetler, S.W., Licciardi, J.M., Teller, J.T., 2001. Freshwater forcing of abrupt climate change during the last glaciation. *Science* 239, 283–287.
- Corliss, B.H., Hunt, A.S., Keigwin Jr., L.D., 1982. Benthonic foraminiferal faunal and isotopic data for the postglacial evolution of the Champlain Sea. *Quaternary Research* 17, 325–338.
- Cronin, T., Rayburn, J., Thunell, R., Guilbault, J.-P., Katz, B., Najjar, R., Manley, P., 2008a. North American Glacial Lake Drainage through the St. Lawrence Estuary from 13 to 9 ka, Fall AGU Meeting 2008 San Francisco, PP51E-05.
- Cronin, T.M., 1977. Late-Wisconsin Marine Environments of the Champlain Valley (New York, Quebec). *Quaternary Research* 7, 238–253.
- Cronin, T.M., 1979. Late Pleistocene benthic foraminifers from the St. Lawrence Lowlands. *Journal of Paleontology* 53, 781–814.
- Cronin, T.M., 1981. Paleoclimate implications of late Pleistocene marine ostracodes from the St. Lawrence Lowlands. *Micropaleontology* 27, 384–418.
- Cronin, T.M., Manley, P.L., Brachfeld, S., Manley, T.O., Willard, D.A., Guilbault, J.-P., Rayburn, J.A., Thunell, R., Berke, M., 2008b. Impacts of post-glacial lake drainage events and revised chronology of the Champlain Sea episode 13–9 ka. *Palaeogeography, Palaeoclimatology, Palaeoecology* 262, 46–60.
- De Simone, D.J., Wall, G.R., Miller, N.G., Rayburn, J.A., Kozlowski, A.L., 2008. Glacial Geology of the Northern Hudson Through Southern Champlain Lowlands. 71st Reunion of the Northeast Friends of the Pleistocene Guidebook 58.
- de Vernal, A., Hillaire-Marcel, C., Bilodeau, G., 1996. Reduced meltwater outflow from the Laurentide ice margin during the Younger Dryas. *Nature* 381, 774–777.
- Dyke, A.S., Moore, A., Robertson, L., 2003. Deglaciation of North America. Geological Survey of Canada, Open File 1574.
- Ellison, C.R.W., Chapman, M.R., Hall, I.R., 2006. Surface and deep ocean interactions during the cold climate event 8200 years ago. *Science* 312, 1929–1932.
- Fairbanks, R.G., 1982. The origin of continental shelf and slope water in the New York Bight and Gulf of Maine: evidence from $\text{H}_2^{18}\text{O}/\text{H}_2^{16}\text{O}$ ratio measurements. *Journal of Geophysical Research* 87, 5796–5808.
- Franzi, D., Rayburn, J., Knuepfer, P., Cronin, T., 2007. Late Quaternary History of Northeastern New York and Adjacent Parts of Vermont and Quebec. 70th Annual Northeast Friends of the Pleistocene Guidebook. Plattsburgh, New York. 70.
- Ganopolski, A., Rahmstorf, S., 2001. Rapid changes of glacial climate simulated in a coupled climate model. *Nature* 409, 153–158.
- Gregory, J.M., Dixon, K.W., Stouffer, R.J., Weaver, A.J., Driesschaert, E., Eby, M., Fichefet, T., Hasumi, H., Hu, A., Jungclaus, J.H., 2005. A model intercomparison of changes in the Atlantic thermohaline circulation in response to increasing atmospheric CO_2 concentration. *Geophysical Research Letters* 32, L12703. doi:10.1029/2005GL023209.
- Guilbault, J.-P., 1989. Foraminiferal distribution in the central and western parts of the Late Pleistocene Champlain Sea Basin, Eastern Canada. *Géographie physique et Quaternaire* 43, 3–26.
- Guilbault, J.-P., 1993. Quaternary foraminiferal stratigraphy in sediments of the eastern Champlain Sea basin, Québec. *Géographie physique et Quaternaire* 47, 43–68.
- Hansen, D.V., Rattray, M., 1965. Gravitational circulation in straits and estuaries. *Journal of Marine Research* 23, 104–122.
- Hillaire-Marcel, C., 1988. Isotopic composition (^{18}O , ^{13}C , ^{14}C) of biogenic carbonates in Champlain Sea sediments. In: Gadd, N.R. (Ed.), *The Late Quaternary Development of the Champlain Sea Basin*, 35. Geological Association of Canada Special Paper, pp. 177–194.
- Hillaire-Marcel, C., Occhietti, S., 1977. Frequency of C-14 dates of marine postglacial fauna in eastern Canada and paleoclimatic changes. *Palaeogeography, Palaeoclimatology, Palaeoecology* 21, 17–54.
- Hoefs, J., 1992. *Stable Isotope Geochemistry*. Springer-Verlag, New York.
- Hofmann, M., Rahmstorf, S., 2009. On the stability of the Atlantic meridional overturning circulation. *PNAS* 106, 20584–20589.
- Hunt, A., Rathburn, A., 1988. Microfaunal assemblages of Southern Champlain Sea piston cores, 35. *The Late Quaternary Development of the Champlain Sea Basin* Geological Association of Canada Special Publication. 145–154.
- Johnson, R.G., McClure, B.T., 1976. A model for Northern Hemisphere continental ice sheet variation. *Quaternary Research* 6, 325–353.

- Koutitonsky, V.G., Navarro, N., Booth, D., 2002. Descriptive physical oceanography of Great-Entry lagoon, Gulf of St. Lawrence. *Estuarine, Coastal and Shelf Science* 54, 833–847.
- LeGrande, A.N., Schmidt, G.A., Shindell, D.T., Field, C.V., Miller, R.L., Koch, D.M., Faluvegi, G., Hoffmann, G., 2006. Consistent simulations of multiple proxy responses to an abrupt climate change event. *Proceedings of the National Academy of Sciences of the United States of America* 103, 837.
- Leverington, D.W., Teller, J.T., 2003. Paleotopographic reconstructions of the eastern outlets of glacial Lake Agassiz. *Canadian Journal of Earth Sciences* 40, 1259–1278.
- Li, M., Zhong, L., Boicourt, W.C., 2005. Simulations of Chesapeake Bay estuary: sensitivity to turbulence mixing parameterizations and comparison with observations. *Journal of Geophysical Research* 110, C12004. doi:10.1029/2004JC002585.
- Licciardi, J.M., Teller, J.T., Clark, P.U., 1999. Freshwater routing by the Laurentide Ice Sheet during the last deglaciation. In: Clark, P.U., Webb, R.S., Keigwin, L.D. (Eds.), *Mechanisms of Global Climate Change at Millennial Time Scales*, Geophysical Monograph, 112. American Geophysical Union, Washington, DC, pp. 177–201.
- Liu, Z., Otto-Bliesner, B.L., He, F., Brady, E.C., Tomas, R., Clark, P.U., Carlson, A.E., Lynch-Stieglitz, J., Curry, W., Brook, E., 2009. Transient simulation of last deglaciation with a new mechanism for Bølling-Allerød warming. *Science* 325, 310–314.
- Lowell, T., Waterson, N., Fisher, T., Loope, H., Glover, K., Comer, G., Hajdas, I., Denton, G., Schaefer, J., Rinterknecht, V., 2005. Testing the Lake Agassiz meltwater trigger for the Younger Dryas. *EOS. Transactions of the American Geophysical Union* 86, 365–373.
- MacCready, P., 2007. Estuarine adjustment. *Journal of Physical Oceanography* 37, 2133–2145.
- Meehl, G.A., Stocker, T.F., Collins, W.D., Friedlingstein, P., Gaye, A.T., Gregory, J.M., Kitoh, A., Knutti, R., Murphy, J.M., Noda, A., Raper, S.C.B., Watterson, I.G., Weaver, A.J., Zhao, Z.-C., 2007. Global climate projections. In: Solomon, S., Qin, D., Manning, M., Chen, Z., Marquis, M., Averyt, K.B., Tignor, M., Miller, H.L. (Eds.), *Climate Change 2007: The Physical Science Basis*. Contribution of Working Group I to the Fourth Assessment Report of the Intergovernmental Panel on Climate Change. Cambridge University Press, Cambridge, United Kingdom and New York, NY, USA, pp. 747–845.
- Meissner, K.J., Clark, P.U., 2006. Impact of floods versus routing events on the thermohaline circulation. *Geophysical Research Letters* 33, L15704. doi:10.1029/2006GL026705.
- Milly, P.C.D., Dunne, K.A., Vecchia, A.V., 2005. Global pattern of trends in streamflow and water availability in a changing climate. *Nature* 438, 347–350.
- Moore Jr., T.C., Walker, J.C.G., Rea, D.K., Lewis, C.F.M., Shane, L.C.K., Smith, A.J., 2000. Younger Dryas interval and outflow from the Laurentide Ice Sheet. *Paleoceanography* 15, 4–18.
- Overpeck, J.T., Otto-Bliesner, B.L., Miller, G.H., Muhs, D.R., Alley, R.B., Kiehl, J.T., 2006. Paleoclimatic evidence for future ice-sheet instability and rapid sea-level rise. *Science* 311, 1747.
- Parent, M., Occhietti, S., 1988. Late Wisconsinan deglaciation and Champlain sea invasion in the St. Lawrence valley, Québec. *Géographie physique et Quaternaire* 42, 215–246.
- Pekárová, P., Miklánek, P., Pekár, J., 2003. Spatial and temporal runoff oscillation analysis of the main rivers of the world during the 19th–20th centuries. *Journal of Hydrology* 274, 62–79.
- Rahmstorf, S., 2002. Rapid climate transitions in a coupled ocean-atmosphere model. *Nature* 372, 82–85.
- Rahmstorf, S., Crucifix, M., Ganopolski, A., Goosse, H., Kamenkovich, I., Knutti, R., Lohmann, G., Marsh, R., Mysak, L.A., Wang, Z., 2005. Thermohaline circulation hysteresis: a model intercomparison. *Geophysical Research Letters* 32, L23605. doi:10.1029/2005GL023655.
- Rawlins, M.A., Steele, M., Holland, M.M., Adam, J.C., Cherry, J.E., Francis, J.A., Groisman, P.Y., Hinzman, L.D., Huntington, T.G., Kane, D.L., Kimball, J.S., Kwok, R., Lammers, R.B., Lee, C.M., Lettenmaier, D.P., McDonald, K.C., Podest, E., Pundsack, J.W., Rudels, B., Serreze, M.C., Shiklomanov, A., Skagseth, Ø, Troy, T.J., Vörösmarty, C.J., Wensnahan, M., Wood, E.F., Woodgate, R., Yang, D., Zhang, K., Zhang, T., 2010. Analysis of the Arctic system for freshwater cycle intensification: observations and expectations. *Journal of Climate* 23, 5715–5737.
- Rayburn, J., Verosub, K., Franzi, D., Knuepfer, P., 2006. A preliminary Paleomagnetic Study of the Glacial Lacustrine/Champlain Sea Transition in Cores from the Northern Champlain Valley. Geological Society of America, New York. Abstracts with Programs, Northeastern Section 38, # 2.
- Rayburn, J.A., Cronin, T.M., Franzi, D.A., Knuepfer, P.L.K., Willard, D.A., 2011. Timing and duration of North American glacial lake discharges and the Younger Dryas climate reversal. *Quaternary Research* 75, 541–551.
- Rayburn, J.A., Knuepfer, P.L., Franzi, D.A., 2005. A series of large, Late Wisconsinan meltwater floods through the Champlain and Hudson Valleys, New York State, USA. *Quaternary Science Reviews* 24, 2410–2419.
- Richard, P.J.H., Occhietti, S., 2005. ¹⁴C chronology for ice retreat and inception of Champlain Sea in the St. Lawrence Lowlands, Canada. *Quaternary Research* 63, 353–358.
- Rodrigues, C.G., 1988. Late Quaternary invertebrate faunal associations and chronology of the western Champlain Sea basin. The Late Quaternary Development of the Champlain Sea Basin. Geological Association of Canada Special Paper 35, 155–176.
- Rodrigues, C.G., 1992. Successions of invertebrate microfossils and the late Quaternary deglaciation of the central St. Lawrence Lowland, Canada and United States. *Quaternary Science Reviews* 11, 503–534.
- Rodrigues, C.G., 2006. Comments on “The Allerød–Younger Dryas–Holocene sequence in the west-central Champlain Sea eastern Ontario: a record of glacial, oceanographic and climatic changes” by U. Brand and F. M. G. McCarthy. *Quaternary Science Reviews*, 24.
- Rodrigues, C.G., Vilks, G., 1994. The impact of glacial lake runoff on the Goldthwait and Champlain Seas: the relationship between glacial Lake Agassiz runoff and the Younger Dryas. *Quaternary Science Reviews* 13, 923–944.
- Saucier, F.J., Chassé, J., 2000. Tidal circulation and buoyancy effects in the St. Lawrence Estuary. *Atmosphere-Ocean* 38, 505–556.
- Schubel, J.R., Pritchard, D.W., 1986. Responses of Upper Chesapeake Bay to variations in discharge of the Susquehanna River. *Estuaries* 9, 236–249.
- Stouffer, R.J., Yin, J., Gregory, J.M., Dixon, K.W., Spelman, M.J., Hurlin, W., Weaver, A.J., Eby, M., Flato, G.M., Hasumi, H., 2006. Investigating the causes of the response of the thermohaline circulation to past and future climate changes. *Journal of Climate* 19, 1365–1387.
- Teller, J.T., Leverington, D.W., 2004. Glacial Lake Agassiz: a 5000 yr history of change and its relationship to the d¹⁸O record of Greenland. *Bulletin of the Geological Society of America* 116, 729–742.
- Teller, J.T., Leverington, D.W., Mann, J.D., 2002. Freshwater outbursts to the oceans from glacial Lake Agassiz and their role in climate change during the last deglaciation. *Quaternary Science Reviews* 21, 879–887.
- Weaver, A.J., Hillaire-Marcel, C., 2004. Global warming and the next ice age. *Science* 304, 400–402.
- Yin, J., Schlesinger, M.E., Stouffer, R.J., 2009. Model projections of rapid sea-level rise on the northeast coast of the United States. *Nature Geoscience* 2, 262–266.